MycoKeys 73: 109–132 (2020)
doi: 10.3897/mycokeys.73.51424
http://mycokeys.pensoft.net

RESEARCH ARTICLE

A peer-reviewed open-access journal
MycoKeys
Launched to accelerate biodiversity research

Four new species of *Trichoderma* in the *Harzianum* clade from northern China

Xin Gu[1,*], Rui Wang[1,*], Quan Sun[1], Bing Wu[2], Jing-Zu Sun[2]

1 *School of Agriculture, Ningxia University, Yinchuan, Ningxia 750021, China* **2** *State Key Laboratory of Mycology, Institute of Microbiology, Chinese Academy of Sciences, No. 3 Park 1, Beichen West Road, Chaoyang District, Beijing 100101, China*

Corresponding author: Jing-Zu Sun (sunjz@im.ac.cn)

Academic editor: T. Lumbsch | Received 24 February 2020 | Accepted 8 September 2020 | Published 8 October 2020

Citation: Gu X, Wang R, Sun Q, Wu B, Sun J-Z (2020) Four new species of *Trichoderma* in the *Harzianum* clade from northern China. MycoKeys 73: 109–132. https://doi.org/10.3897/mycokeys.73.51424

Abstract

The *Harzianum* clade of *Trichoderma* comprises many species, which are associated with a wide variety of substrates. In this study, four new species of *Trichoderma*, namely *T. lentinulae*, *T. vermifimicola*, *T. xixiacum*, and *T. zelobreve*, were encountered from a fruiting body and compost of *Lentinula*, soil, and vermicompost. Their colony and mycelial morphology, including features of asexual states, were described. For each species, their DNA sequences were obtained from three loci, the internal transcribed spacer (ITS) regions of the ribosomal DNA, the gene encoding the second largest nuclear RNA polymerase subunit (RPB2), the translation elongation factor 1-α encoding gene (TEF1-α). The analysis combining sequences of the three gene regions distinguished four new species in the *Harzianum* clade of *Trichoderma*. Among them, *T. lentinulae* and *T. xixiacum* clustered with *T. lixii*, from which these new species differ in having shorter phialides and smaller conidia. Additionally, *T. lentinulae* differs from *T. xixiacum* in forming phialides with inequilateral to a strongly-curved apex, cultural characteristics, and slow growth on PDA. *Trichoderma vermifimicola* is closely related to *T. simmonsii*, but it differs from the latter by producing phialides in verticillate whorls and smaller conidia. *Trichoderma zelobreve* is the sister species of *T. breve* but is distinguished from *T. breve* by producing shorter and narrower phialides, smaller conidia, and by forming concentric zones on agar plates. This study updates our knowledge of species diversity of *Trichoderma*.

Keywords

compost, fungicolous, Hypocreaceae, mycoparasite

* Authors contributed equally to this work

Copyright *Xin Gu et al.* This is an open access article distributed under the terms of the Creative Commons Attribution License (CC BY 4.0), which permits unrestricted use, distribution, and reproduction in any medium, provided the original author and source are credited.

Introduction

The genus *Trichoderma* Pers., introduced by Persoon (1794), is cosmopolitan, including saprotrophs and mycoparasites in a diversity of ecosystems, such as agricultural fields, prairies, forests, salt marshes, and fungal fruiting body (Gazis and Chaverri 2010; Chaverri et al. 2015; Qiao et al. 2018). Species of this genus have been widely used in the biocontrol of plant pathogens (Chaverri et al. 2015; Degenkolb et al. 2015; Bunbury-Blanchette and Walke 2019) and production of enzymes and bioactive compounds (Sun et al. 2016). Nevertheless, some of them are associated with green mold diseases in the commercial production of mushrooms (Innocenti et al. 2019; Sun et al. 2019a). Morphologically, the asexual-morphs are similar in producing branched tree-like conidiophores with cylindrical to nearly subglobose phialides and ellipsoidal to globose conidia, but their variation is insufficient to differentiate the *Trichoderma* species (Chaverri et al. 2015; Qin and Zhuang 2017; Qiao et al. 2018). Multilocus molecular phylogeny, based on combined sequence data of the internal transcribed spacer (ITS) regions, RNA polymerase II subunit (RPB2), and the translation elongation factor 1-α gene (TEF1-α), enables rapid and accurate identification of the *Trichoderma* species (Druzhinina et al. 2005; Atanasova et al. 2013; Chaverri et al. 2015). Currently, the combination of multi-gene phylogenetic analysis and phenotypic characteristics is extensively applied in species delimitation of *Trichoderma* (du Plessis et al. 2018; Qiao et al. 2018; Innocenti et al. 2019).

Trichoderma harzianum Rifai is one of the most well-known *Trichoderma* species, due to its antifungal properties and effective bio-control ability, used to suppress soil-borne plant pathogens (Chaverri et al. 2015; Degenkolb et al. 2015; Bunbury-Blanchette and Walker 2019). As a cosmopolitan and ubiquitous fungus, it has been isolated from diverse substrates, such as soil, plant tissue, and mushrooms (Chaverri et al. 2015; Jaklitsch and Voglmayr 2015; Innocenti et al. 2019; Sun et al. 2019b). Since Chaverri et al. (2015) provided a systematic revision of species in the *Harzianum* clade, numerous new species have been described (Jaklitsch and Voglmayr 2015; Qin and Zhuang 2016a; Sun et al. 2016; Chen and Zhuang 2017b; Qiao et al. 2018). Currently, more than 60 species are placed in the *Harzianum* clade (Jaklitsch and Voglmayr 2015; Qin and Zhuang 2016a, b, 2017; Chen and Zhuang 2017b; Qiao et al. 2018; Phookamsak et al. 2019;).

It is estimated that 136 new species of *Trichoderma* have been recognised since 2015 (www.indexfungorum.org 2020), with 84 among these reported from China (Sun et al. 2012; Qin and Zhuang 2016a, b, 2017; Chen and Zhuang 2017a, b; Qiao et al. 2018), which evidenced that China has a high species diversity of *Trichoderma* (Zhu and Zhuang 2015; Jiang et al. 2016). In our survey of *Trichoderma*, eighteen isolates were obtained from soil, mushroom substrates, and vermicompost from northern China. Four new species belonging to the *Harzianum* clade were identified based on morphological features and DNA sequence data at three loci: the genes encoding RNA polymerase II subunit (RBP2) and translation elongation factor 1-α gene (TEF1-α), and the internal transcribed spacer (ITS) regions of the nuclear ribosomal RNA gene.

Materials and methods

Sampling sites and strains isolation

Since *Trichoderma* is easily isolated from soil, mushroom substrates, and earthworm substrates, the soil, mushroom substrates, and earthworm were therefore collected from Yinchuan, Ningxia Hui Autonomous Region, and Chaoyang district, Beijing, China. All the samples were stored at 4 °C before fungal isolation. *Trichoderma* strains were isolated by gradient dilution and the spread plate method or directly from the mushroom substrates. Three dilutions (10^{-1}, 10^{-2}, and 10^{-3}) were prepared with 1 g soil and sterile water, and 100 μl of each dilution was spread on a 9 cm diameter Petri dish of PDA agar with100 mg/L chloramphenicol added. The plates were then incubated at 25 °C. Each of the individual colonies was transferred to a new PDA dish after 1–3 days and incubated at 25 °C. Dried cultures from the single spore or specimens of new species were deposited in the Herbarium Mycologicum Academiae Sinicae (HMAS) and the ex-type strains were preserved in the China General Microbiological Culture Collection Center (CGMCC)

Morphological analysis

For morphological studies, we used three different media: cornmeal dextrose agar (CMD, Difco, BD Science, USA), PDA (Difco, BD Science, USA), and synthetic low nutrient agar (SNA, Difco, BD Science, USA) (Chaverri et al. 2015). Each strain was first cultured on an SNA plate for 3 days and a small agar piece of 0.5 cm diameter with mycelium was then transferred, respectively, to new CMD, PDA, and SNA plates. Strains were incubated in 9 cm diam with three replicates. Petri dishes at 25 °C with a 12 h natural light and 12 h darkness interval. Colony diameter at 25 °C was measured three days after inoculation, and the time when mycelium entirely covered the surface of the agar plate was also recorded. Micromorphological characters were examined from the cultures of one-week-old colonies on SNA (Chaverri et al. 2015). A Nikon Ellipse 80i light microscope, equipped with differential interference contrast (DIC) optics, was used to capture digital images.

DNA extraction, PCR and sequencing

Genomic DNA of each strain was extracted from fresh mycelium growing on PDA after 5 days of growth following the rapid "thermolysis" method described in Zhang et al. (2010). For the amplification of ITS, RPB2, and TEF1-α gene fragments, ITS4 and ITS5 for ITS (White et al. 1990), EF1-728F (Carbone and Kohn 1999) and TEF1LLErev (Jaklitsch et al. 2005) for TEF1, and RPB2-5F and RPB2-7R for rpb2 (Liu et al. 1999) were used. Each PCR reaction consisted of 12.5 μl T5

Super PCR Mix (containing Taq polymerase, dNTP, and Mg^{2+}, Beijing TsingKe Biotech Co. Ltd., Beijing), 1.0 μl of forward primer (10 μM), 1.0 μl of reverse primer (10 μM), 0.5 μl DMSO, 3 μl DNA template and 7 μl double sterilized water. PCR reactions were in Eppendorf Mastercycler, following the protocols described by Sun et al. (2016). PCR products were purified with the PCR product purification kit (TIANGEN Biotech, Beijing, China), and sequencing was carried out in both directions on an ABI 3730 XL DNA sequencer (Applied Biosystems, Foster City, California) with primers used during PCR amplification.

Phylogenetic analyses

Preliminary BLAST searches with ITS, RPB2, and TEF1-α gene sequences of the new isolates against NCBI, TrichOKey (Druzhinina and Kopchinski 2006), and TrichoBlast (Kopchinskiy et al. 2005) databases identified species closely related to our isolates. Based on this information, sequences of ITS, RBP2, and TEF1-α of 133 strains, representing 59 species were downloaded from GenBank, following recent publications (Qin and Zhuang 2017; Qiao et al. 2018; Innocenti et al. 2019). Among them, 139 strains are belonging to the *Harzianum* clade, and *Trichoderma ceramicum*, *T. parestonicum*, and *T. estonicum* were chosen to represent the outgroup.

Tree alignment files were generated by using MAFFT version 7.03 with the Q-INS-I strategy (Katoh and Standley 2013). Conserved blocks were selected from the initial alignments with Gblocks 0.91 b (Castresana 2000). The appropriate nucleotide substitution model for each gene was determined by using MrModeltest v2.4 (Nylander 2004). HKY + I + G was estimated as the best-fit model for RPB2, and GTR + I + G was estimated as the best-fit model for TEF1-α and ITS under the output strategy of AIC. The partition homogeneity test ($p = 0.01$) indicated that the individual partitions were not significantly incongruent (Cunningham 1997), thus the aligned sequences of ITS, RPB2, and TEF1-α were combined for analyses. The multi-locus phylogenetic analyses included 1065 characters for RBP2, 587 characters for TEF1-α, and 555 characters for ITS. All characters were weighted equally and gaps were treated as missing characters.

Maximum Likelihood (ML) analyses were performed by RAxML (Stamatakis 2006), using the GTR-GAMMA-I model. The maximum likelihood bootstrap proportions (MLBP) were using 1000 replicates. Bayesian Inference (BI) analyses were conducted with MrBayes v3.2.6 (Ronquist et al. 2012). Metropolis-coupled Markov Chain Monte Carlo (MCMC) searches were calculated for 10,000,000 generations, sampling every 100th generation with the best best-fit model for each gene. Two independent analyses with six chains each (one cold and five heated) were carried out until the average standard deviation of the split frequencies dropped below 0.01. The initial 25% of the generations of MCMC sampling were discarded as burn-in. The refinement of the phylogenetic tree was used for estimating Bayesian

inference posterior probability (PP) values. The Tree was viewed in FigTree v1.4 (Rambaut 2012), values of Maximum likelihood bootstrap proportions (MLBP) greater than 50% and Bayesian inference posterior probabilities (BIPP), greater than 95% at the nodes, are shown along branches. The final alignments and the trees obtained have been deposited in TreeBASE (TreeBASE accession number: 25400).

Results

Phylogeny

The preliminary BLAST searches with ITS, RPB2, and TEF1-α gene sequences of the new isolates suggest our isolates were highly similar to species from *Trichoderma* in the *Harzianum*-complex. Therefore, as the next step phylogenetic analyses were conducted by using a single gene of ITS, RPB2, TEF1-α, and multi-gene dataset of cascaded ITS, RPB2, and TEF1-α, respectively. The phylogenetic trees showed that our isolates were placed in the *Harzianum* clade (Fig. 1, Suppl. material 1: Fig. S1, Suppl. material 2: Fig. S2, Suppl. material 3: Fig. S3). In the phylogenetic tree conducted by a combined matrix of ITS, RPB2, and TEF1-α sequences, isolates of *T. lentinulae*, *T. xixiacum*, and *T. lixii* formed a well-supported clade (MLBP/BIBP = 73%/1.00). Within this clade, isolates of *T. lentinulae* and *T. xixiacum* formed a subclade with maximum support. Isolates of *T. vermifimicola* clustered together with *T. simmonsii* (BIBP = 1.00), both forming a subclade with maximum support (MLBP/BIBP = 100%/1.00, Fig. 1). *Trichoderma zelobreve* and *T. breve*, were distinguished by maximum support to respective clades while forming a highly supported clade (MLBP/BIBP = 100%/1.00, Fig. 1).

The ITS gene could not distinguish our isolates from other species within the *Harzianum* clade (Suppl. material 1: Fig. S1). In the phylogenetic tree resulted from the RPB2 gene, *Trichoderma lentinulae*, *T. xixiacum*, and *T. lixii* formed a highly supported clade (MLBP/BIBP = 100%/1.00), but within this clade, *T. lentinulae*, *T. xixiacum* were not distinguished (Suppl. material 2: Fig. S2). Isolates of *T. vermifimicola* formed a distinct clade (MLBP/BIBP = 100%/1.00) and grouped with *T. simmonsii*, *T. guizhouense*, and *T. rugulosum* but weakly supported (Suppl. material 3: Fig. S3). *Trichoderma zelobreve* and *T. breve* also formed a highly supported clade (MLBP/BIBP = 98%/1.00), but *T. zelobreve* and *T. breve*, were distinguished by maximum support to respective clades while forming a highly supported clade (MLBP/BIBP = 100%/1.00, Suppl. material 2: Fig. S2). In the phylogenetic tree resulted from the TEF1-α gene, *T. zelobreve* and *T. breve* also formed a highly supported clade (MLBP/BIBP = 98%/1.00), but were not distinct from each other (Suppl. material 3: Fig. S3). Isolates of *T. lentinulae*, *T. xixiacum*, *T. vermifimicola*, and *T. simmonsii* clustered together but this clade was not well-supported. Within this clade, isolates of *T. lentinulae* formed a well-supported subclade (MLBP/

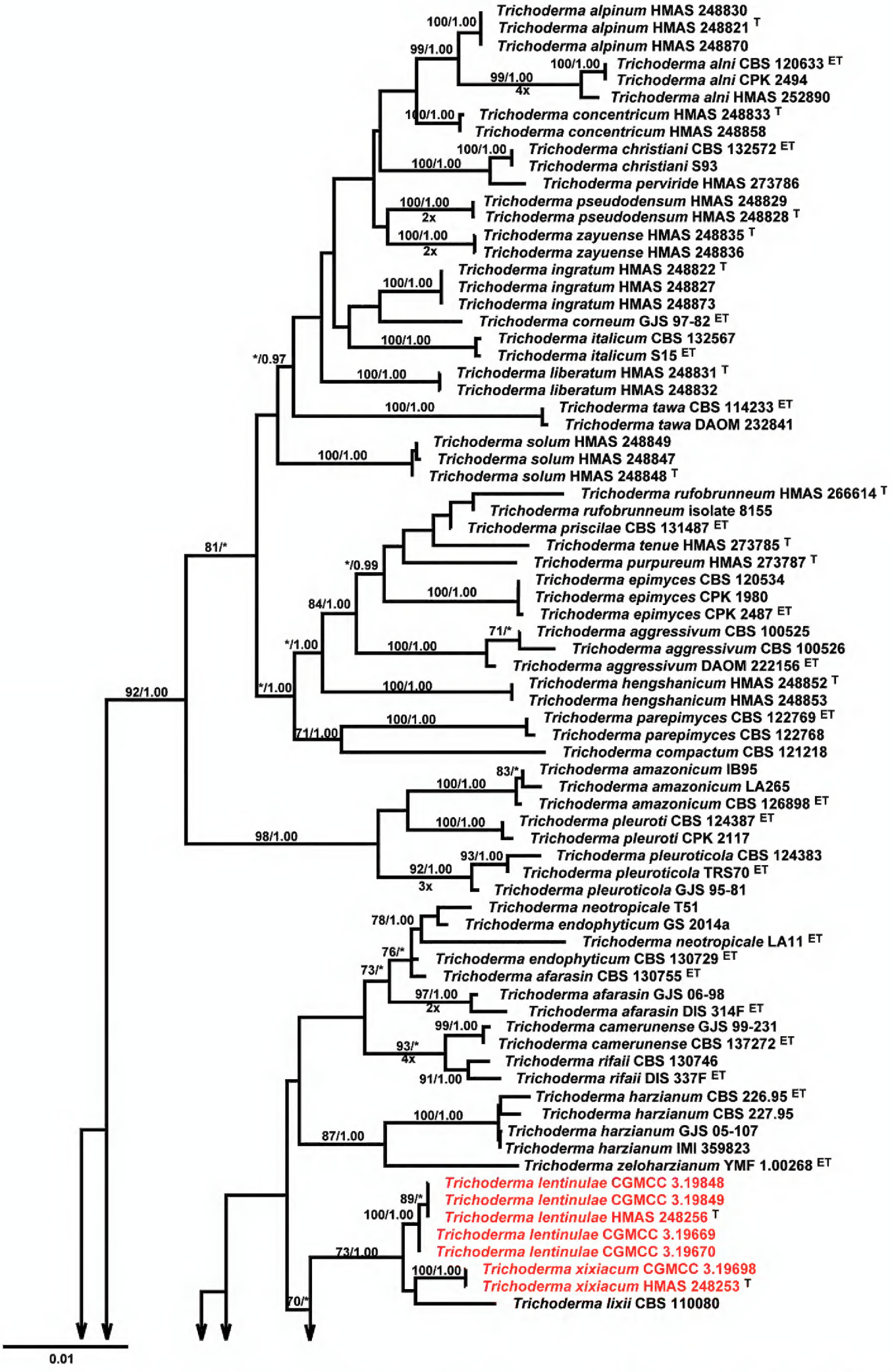

Figure 1. Phylogenetic tree based on Maximum Likelihood analysis of a combined ITS, RPB2, and TEF1α sequence dataset. *Trichoderma estonicum*, *Trichoderm parastinicum*, *Trichoderm ceramicum* were chosen as the outgroup. Bootstrap Values higher than 70% from RAxML (BSML) (left) and Bayesian posterior probabilities greater than 0.95 (BYPP) (right) are given above the nodes. ^{T} indicates the type; ^{ET} indicates the ex-living type. Isolates obtained in this study are in red.

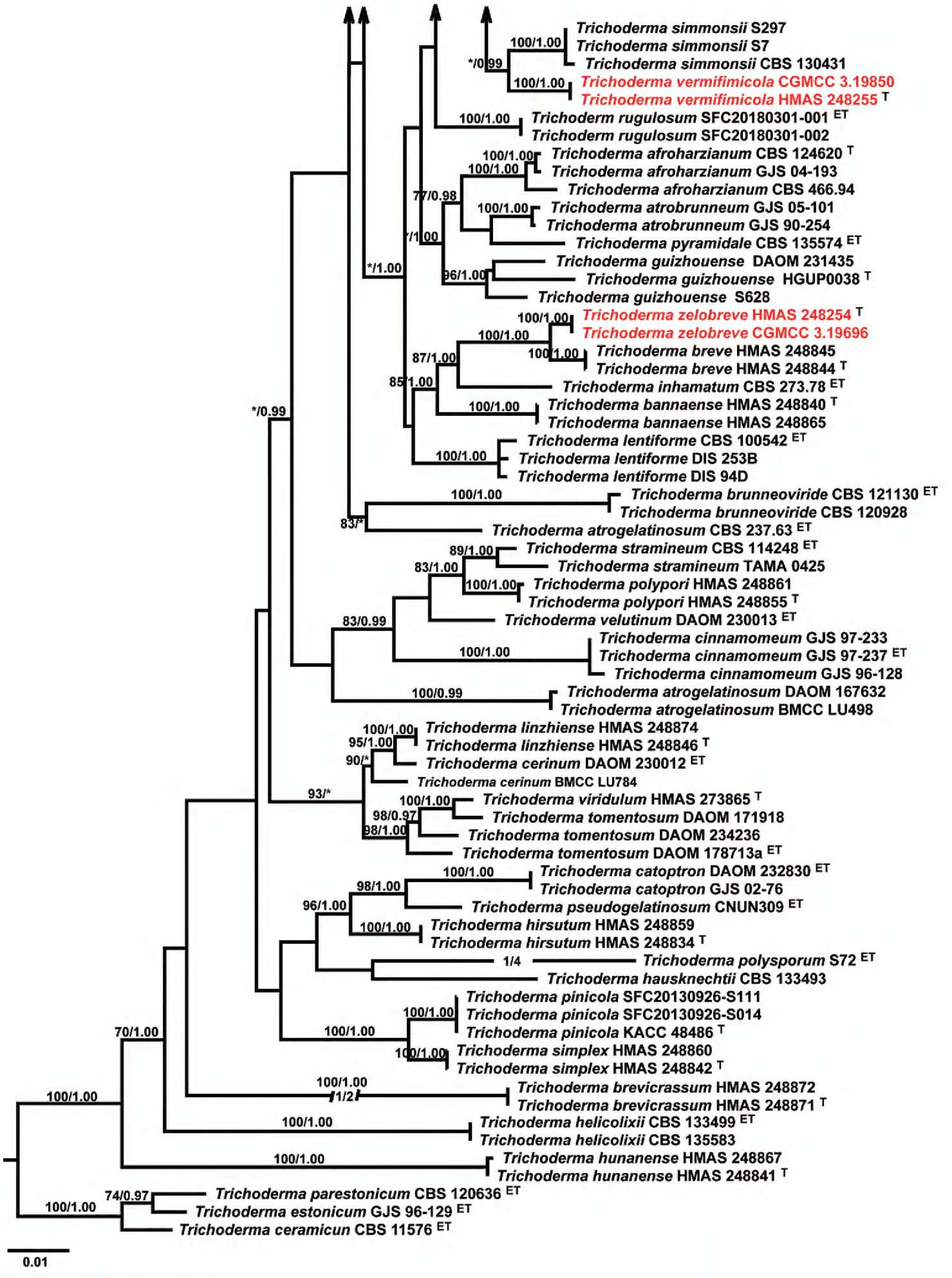
Trichoderma simmonsii S297
Trichoderma simmonsii S7
Trichoderma simmonsii CBS 130431
Trichoderma vermifimicola CGMCC 3.19850
Trichoderma vermifimicola HMAS 248255 T
Trichoderm rugulosum SFC20180301-001 ET
Trichoderm rugulosum SFC20180301-002
Trichoderma afroharzianum CBS 124620 T
Trichoderma afroharzianum GJS 04-193
Trichoderma afroharzianum CBS 466.94
Trichoderma atrobrunneum GJS 05-101
Trichoderma atrobrunneum GJS 90-254
Trichoderma pyramidale CBS 135574 ET
Trichoderma guizhouense DAOM 231435
Trichoderma guizhouense HGUP0038 T
Trichoderma guizhouense S628
Trichoderma zelobreve HMAS 248254 T
Trichoderma zelobreve CGMCC 3.19696
Trichoderma breve HMAS 248845
Trichoderma breve HMAS 248844 T
Trichoderma inhamatum CBS 273.78 ET
Trichoderma bannaense HMAS 248840 T
Trichoderma bannaense HMAS 248865
Trichoderma lentiforme CBS 100542 ET
Trichoderma lentiforme DIS 253B
Trichoderma lentiforme DIS 94D
Trichoderma brunneoviride CBS 121130 ET
Trichoderma brunneoviride CBS 120928
Trichoderma atrogelatinosum CBS 237.63 ET
Trichoderma stramineum CBS 114248 ET
Trichoderma stramineum TAMA 0425
Trichoderma polypori HMAS 248861
Trichoderma polypori HMAS 248855 T
Trichoderma velutinum DAOM 230013 ET
Trichoderma cinnamomeum GJS 97-233
Trichoderma cinnamomeum GJS 97-237 ET
Trichoderma cinnamomeum GJS 96-128
Trichoderma atrogelatinosum DAOM 167632
Trichoderma atrogelatinosum BMCC LU498
Trichoderma linzhiense HMAS 248874
Trichoderma linzhiense HMAS 248846 T
Trichoderma cerinum DAOM 230012 ET
Trichoderma cerinum BMCC LU784
Trichoderma viridulum HMAS 273865 T
Trichoderma tomentosum DAOM 171918
Trichoderma tomentosum DAOM 234236
Trichoderma tomentosum DAOM 178713a ET
Trichoderma catoptron DAOM 232830 ET
Trichoderma catoptron GJS 02-76
Trichoderma pseudogelatinosum CNUN309 ET
Trichoderma hirsutum HMAS 248859
Trichoderma hirsutum HMAS 248834 T
Trichoderma polysporum S72 ET
Trichoderma hausknechtii CBS 133493
Trichoderma pinicola SFC20130926-S111
Trichoderma pinicola SFC20130926-S014
Trichoderma pinicola KACC 48486 T
Trichoderma simplex HMAS 248860
Trichoderma simplex HMAS 248842 T
Trichoderma brevicrassum HMAS 248872
Trichoderma brevicrassum HMAS 248871 T
Trichoderma helicolixii CBS 133499 ET
Trichoderma helicolixii CBS 135583
Trichoderma hunanense HMAS 248867
Trichoderma hunanense HMAS 248841 T
Trichoderma parestonicum CBS 120636 ET
Trichoderma estonicum GJS 96-129 ET
Trichoderma ceramicun CBS 11576 ET
0.01

Figure 1. Continued.

BIBP = 91%/1.00). *Trichoderma xixiacum* and *T. vermifimicola* formed a highly supported subclade (MLBP/BIBP = 100%/1.00). Within this group, isolates of *T. vermifimicola* clustered together with well-supported (MLBP/BIBP = 93%/1.00, Suppl. material 3: Fig. S3).

Taxonomy

***Trichoderma lentinulae* Jing Z. Sun & X.Z. Liu, sp. nov.**
MycoBank No: 833233
Fig. 2

Etymology. Latin, *lentinulae*, refers to the host from which the fungus was isolated.

Type. China. Haidian District, Beijing, 39°57'40"N, 116°19'40"E, ca. 27 m elev., from a fruiting body and mushroom spawn of *Lentinula edodes*, 19 Oct 2018, Jing Z. Sun (HMAS 248256, holotype), ex-type culture CGMCC 3.19847.

Description. On CMD after 72 h, colony radius 57–58 mm at 25 °C, covering the plate at 30 °C, 4–5 mm at 35 °C. Colony hyaline, weak, indistinctly radial. Aerial hyphae short, inconspicuous. No diffusing pigment noted, odor indistinct (Fig. 2B). Conidial production noted after 3 days, scant, effuse in aerial hyphae, becoming blue-green after 7 days. Chlamydospores not observed.

On PDA after 72 h, colony radius 45–46 mm at 25 °C, mycelium covering the plate at 30 °C, 11–12 mm at 35 °C. Colony white to yellowish-white, regularly circular, indistinctly zonate; mycelium dense and radial. No diffusing pigment, not distinct odor (Fig. 2A). Conidial production noted after 3 days, starting around the original inoculum, effuse in the aerial hyphae, first white, turning green after 3 d. Chlamydospores unobserved.

On SNA after 72 h, colony radius 51–52 mm at 25 °C, 52–53 mm at 30 °C, 4–5 mm at 35 °C. Colony hyaline, indistinctly zonate; mycelium loose, especially at the margin. Aerial hyphae loose. No diffusing pigment, not distinct odor (Fig. 2C). Conidial production noted after 2 days, starting around the inoculum, effuse in the aerial hyphae. Small pustules formed around the inoculum, first white, turning green after 3 d, with hairs protruding beyond the surface. Conidiophores pyramidal with opposing branches, less frequently solitary, closely-spaced branches, each branch, and the main axis terminating in 2–5 cruciately to nearly verticillately disposed phialides (Fig. 2F, H, I). Phialides ampulliform, typically strongly constricted below the tip, less frequently lageniform and then usually apex and inequilateral to strongly curved, hyaline, (3.5–)4.0–6.0(–6.5) × (2.0–)2.5–3.0(–3.5) µm ($\bar{x}$ = 4.5 × 3.0 µm, n = 30), length/width ratio (1.5–)2.0–3.0(–5.0) ($\bar{x}$ = 2.0, n = 30), base 1.0–2.5 µm ($\bar{x}$ = 1.5 µm)(Fig. 2G, H, I). Conidia ovoid to globose, smooth, hyaline when young, becoming green to dark green with age, (2.0–)2.5–3.0(–3.5) × (1.5–)2.0–2.5(–3.0) µm ($\bar{x}$ = 2.5 × 2.2 µm, n = 50), length/width ratio (1.0–)1.1–1.4 (–1.5) ($\bar{x}$ = 1.2, n = 50) (Fig. 2J). Chlamydospores common, apex or intercalary, ellipsoid or subglobose, (3.5–)5.0–6.5(–7.0) × (3.0–)4.0–5.0(–6.0) µm ($\bar{x}$ = 5.5 × 4.5 µm, n = 30), length/width ratio (1.0–)1.2–1.5 (–1.7) ($\bar{x}$ = 1.2, n = 30) (Fig. 2K–M).

Additional specimen examined. China. Haidian District, Beijing, 39°57'40"N, 116°19'40"E, ca. 27 m elev., From a fruiting body and mushroom spawn of *Lentinula edodes*, 19 Oct 2018, Jing Z. Sun, living culture CGMCC 3.19848; Xixia District, Yinchuan, Ningxia Hui Autonomous Region, 38°38'52"N, 106°9'33"E, ca. 1127 m elev., from rhizosphere soil of Lycium chinois, 17 Oct 2018, Jing Z. Sun, living culture CGMCC 3.19699; ibid., living culture CGMCC 3.19670.

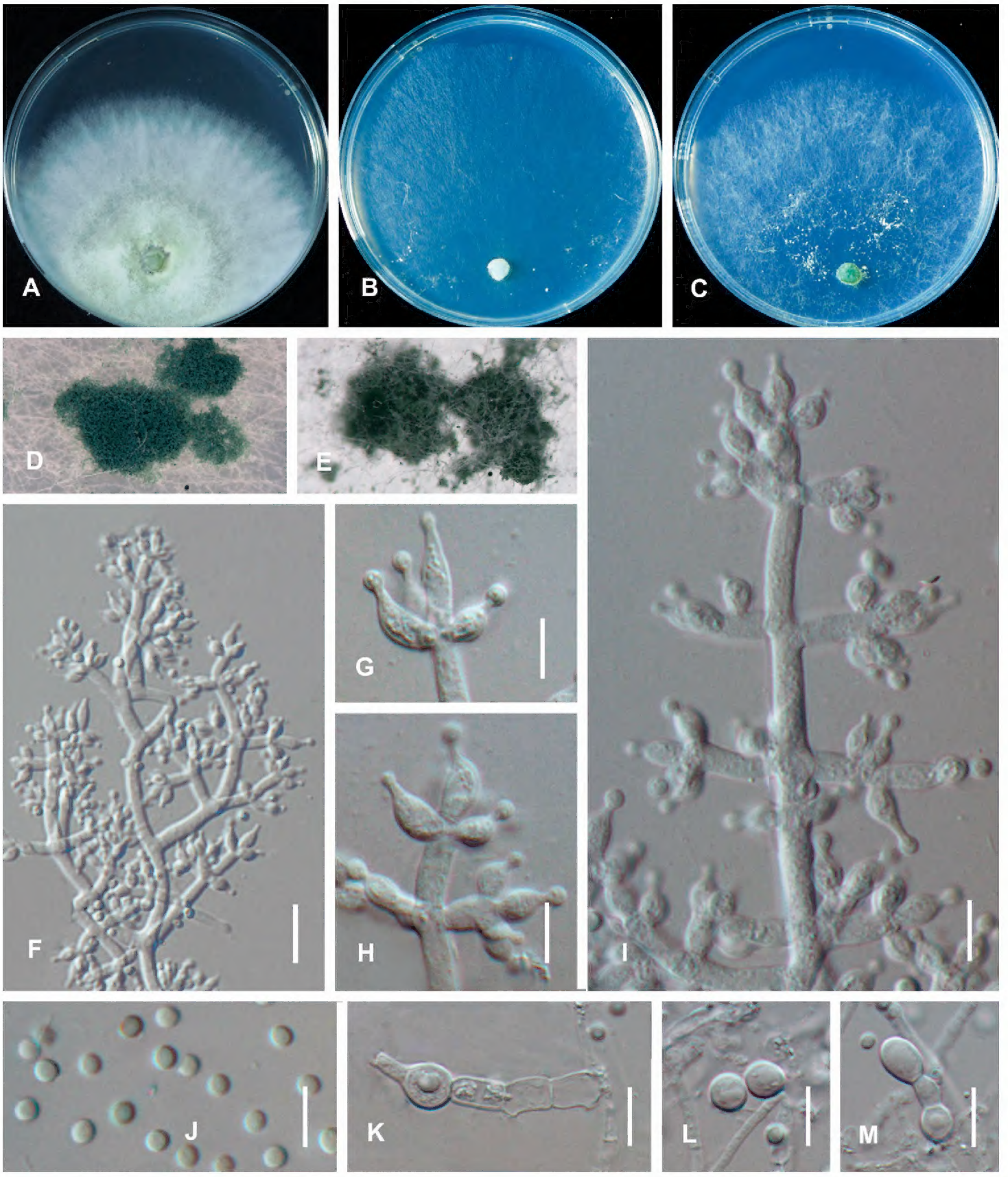

Figure 2. *Trichoderma lentinulae* (CGMCC 3.19847). Cultures at 25 °C after 3 days (**A** on PDA **B** on CMD **C** on SNA) **D** conidiation pustules on CMD after 10 days **E** conidiation pustules on CMD after 10 d **F** conidiophores **G–I** Conidiophores and phialides **J** conidia **K–M** chlamydospores. Scale bars: 25 μm (**F**); 10 μm (**G–M**).

Teleomorph. Undetermined.

Note. The species is characterized by tree-like conidiophores, phialides verticillate or in whorls of 3–4, spindle-like to fusiform phialides (4.0–6.0 × 2.5–3.0 μm) and ovoid to subglobose conidia. Differs from *T. lixii* by shorter and wider phialides and smaller conidia. Differs from *Trichoderma xixiacum* by compact, relatively smaller phialides, and the pustules not forming distinctly zonate of pustules on SNA.

Trichoderma vermifimicola **Jing Z. Sun & X.Z. Liu, sp. nov.**
MycoBank No: 833234
Fig. 3

Etymology. Latin, *vermifimicola*, refers to the habitat of the type species.

Type. China. Yongning, Yinchuan, the Ningxia Hui Autonomous Region, 40°0'41"N, 116°23'37"E, ca. 1678 m elev., from the substrates for earthworm cultivation, 18 Oct 2018, Jing Z. Sun (HMAS 248255, holotype), ex-type culture CGMCC 3.19694.

Description. On CMD after 72 h, colony radius 49–51 mm at 25 °C, 51–52 mm at 30 °C, 4–5 mm at 35 °C. Colony hyaline, irregularly circular, indistinctly zonate; mycelium loose. Aerial hyphae short, inconspicuous. No diffusing pigment, not distinct odor. Conidial production noted after 3 days, starting around the inoculum (Fig. 3B). Small pustules formed at the colony margin, first white, turning blue-green after 7 d, with hairs protruding beyond the surface. Chlamydospores unobserved.

On PDA after 72 h, colony radius 55–58 mm at 25 °C, 55–56 mm at 30 °C, 5–6 mm at 35 °C. Colony white-green to bright green, regularly circular, distinctly zonate; mycelium dense and radial. Aerial hyphae short, inconspicuous. No diffusing pigment, not distinct odor. Conidial production noted after 2 days, starting around the inoculum, effuse in the aerial hyphae, first white, turning green after 2 d (Fig. 3A). Chlamydospores unobserved.

On SNA after 72 h, colony radius 48–50 mm at 25 °C, 51–52 mm at 30 °C, 3–4 mm at 35 °C. Colony hyaline, regularly circular, distinctly zonate; mycelium loose, especially at the margin. Aerial hyphae short, inconspicuous. No diffusing pigment, not distinct odor. Conidial production noted after 2 days, starting around the inoculum, effuse in the aerial hyphae. Small pustules formed along with two concentric rings, first white, turning yellow-green after 3 d, with hairs protruding beyond the surface (Fig. 3C). Conidiophores pyramidal with opposing branches, the distance between branches relatively large, each branch terminating in a whorl of 2–3 phialides, phialides sometimes solitary on the main axis (Fig. 3F, H, K); whorls typically cruciate, but often nearly verticillate (Fig. 3K); rarely conidiophores nodose and phialides disposed in more or less botryose clusters (Fig. 3H). Phialides ampulliform to lageniform, often constricted below the tip to form a narrow neck, hyaline, (4.4–)5.0–10.5(–11.2) × (2.0–)2.5–3.0(–3.5) µm ($\bar{x}$ = 6.6 × 2.7 µm, n = 30), length/width ratio (1.5–)1.8–2.8(–5.3) ($\bar{x}$ = 2.4, n = 30), base 1.6–2.5 µm ($\bar{x}$ = 1.9 µm) (Fig. 3G, I, K). Conidia ovoid to subglobose, smooth, hyaline when young, becoming green to dark green with age, (2.0–)2.3–2.6(–3.0) × (1.5–)2.0–2.4(–2.8) µm ($\bar{x}$ = 2.4 × 2.2 µm, n = 50), length/width ratio (1.0–)1.1–1.4(–1.7) ($\bar{x}$ = 1.2, n = 50) (Fig. 3J). Chlamydospores unobserved. No odor; no diffusing pigment observed.

Additional specimen examined. China. Xixia District, Yinchuan, Ningxia Hui Autonomous Region, 38°38'52"N, 106°9'33"E, ca. 1127 m elev., from rhizosphere soil of Lycium chinois, 17 Oct 2018, Jing Z. Sun, living CGMCC 3.19697.

Teleomorph. Undetermined.

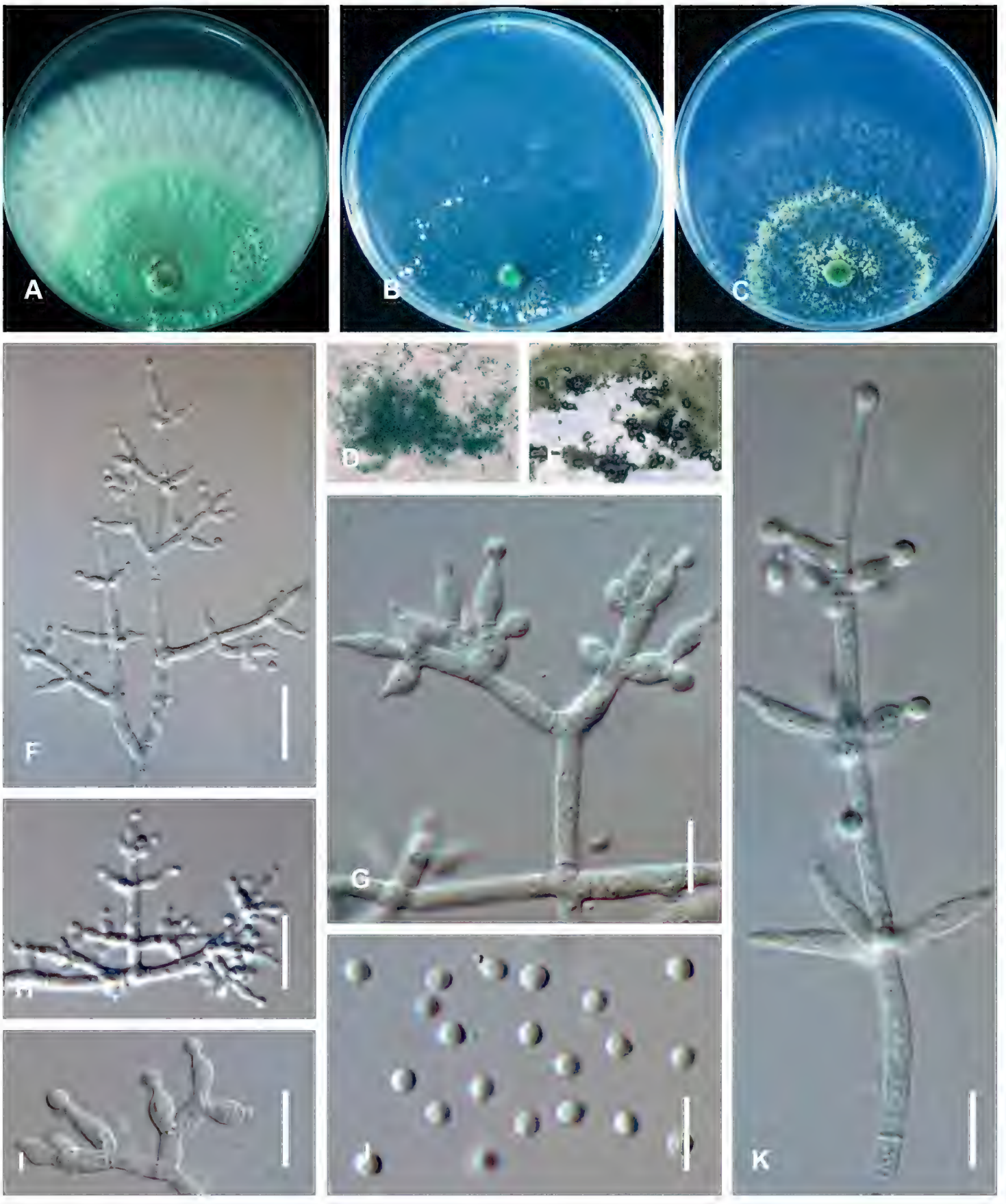

Figure 3. *Trichoderma vermifimicola* (CGMCC 3.19694). Cultures at 25 °C after 3 days (**A** on PDA **B** on CMD **C** on SNA) **D** conidiation pustules on CMD after 10 days **E** conidiation pustules on SNA after 10 d **F, H** conidiophores **G, J, K** conidiophores and phialides **I** conidia. Scale bars: 25 μm (**F, H**); 10 μm (**G, J–K**).

Note. Characterized by tree-like conidiophores, verticillate or in whorls of 3–4, ampulliform to lageniform phialides (5.0–10.5 × 2.5–3.0 μm), ovoid to subglobose conidia (2.4–2.6 × 2.0–2.5 μm). Differs from *Trichoderma simmonsii* by forming loose branches in whorls, relatively longer and thinner phialides, smaller conidia, and the fewer pustules on SNA.

Trichoderma xixiacum **Jing Z. Sun & X.Z. Liu, sp. nov.**
MycoBank No: 833235
Fig. 4

Etymology. Latin, *xixiacum*, refers to the type locality.

Type. China. Xixia District, Yinchuan, Ningxia Hui Autonomous Region, 38°38'52"N, 106°9'33"E, ca. 1127 m elev., from rhizosphere soil of *Lycium chinois*, 17 Oct 2018, Jing Z. Sun (HMAS 248253, holotype), ex-type culture CGMCC 3.19697.

Description. On CMD after 72 h, colony radius 55–56 mm at 25 °C, covering the plate at 30 °C, 9–11 mm at 35 °C. Colony hyaline, indistinctly zonate, mycelia loose. Aerial hyphae short, inconspicuous. No diffusing pigment, not distinct odor (Fig. 4B). Conidial production noted after 3 days, effuse in aerial hyphae, becoming blue-green after 4 days. Chlamydospores unobserved.

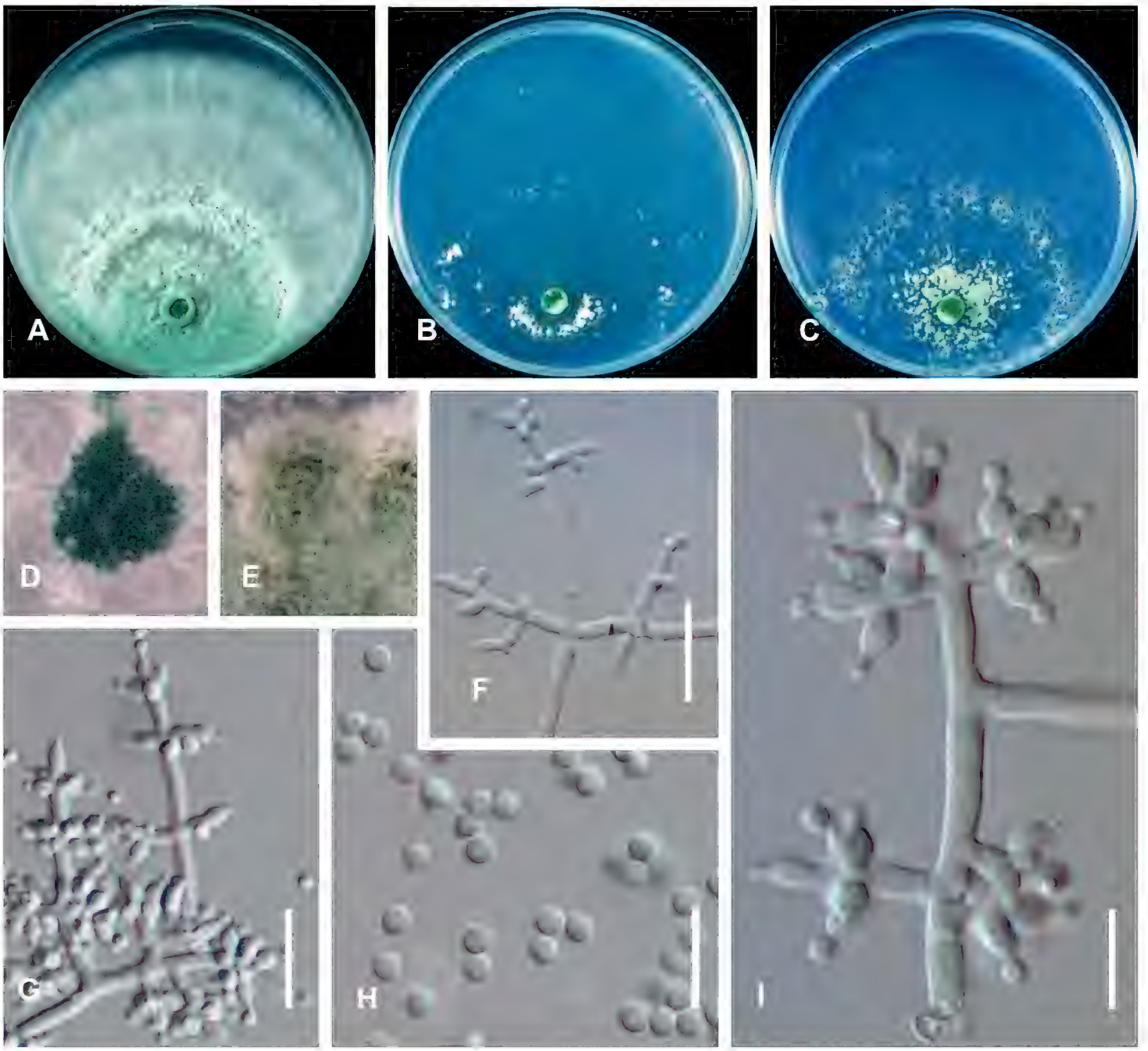

Figure 4. *Trichoderma xixiacum* (CGMCC 3.19697). Cultures at 25 °C after 3 d (**A** on PDA **B** on CMD **C** on SNA) **D** conidiation pustules on CMD after 10 d **E** conidiation pustules on SNA after 10 d **F, G, I** conidiophores and phialides **H** conidia. Scale bars: 10 μm (**F, G**); 10 μm (**H, I**).

On PDA after 72 h, colony radius 59–60 mm at 25 °C, covering the plate at 30 °C, 7–8 mm at 35 °C. Colony white to yellow-white, regularly circular, indistinctly zonate; mycelium dense and radial. Aerial hyphae conspicuous. No diffusing pigment, not distinct odor (Fig. 4A). Conidial production noted after 3 days, starting around the original inoculum, effuse in the aerial hyphae, first white, turning blue-green after 7 d. Chlamydospores unobserved.

On SNA after 72 h, colony radius 51–52 mm at 25 °C, 52–53 mm at 30 °C, 4–5 mm at 35 °C. Colony hyaline, indistinctly zonate; mycelium loose, especially at the margin. Aerial hyphae short. No diffusing pigment, not distinct odor (Fig. 4C). Conidial production noted after 2 days, starting around the inoculum, effuse in the aerial hyphae. Small pustules formed around the inoculum, first white, turning green after 3 d, with hairs protruding beyond the surface. Conidiophores pyramidal with opposing branches, less frequently solitary, closely-spaced branches, each branch, and the main axis terminating in 2–5 cruciately to nearly verticillately disposed phialides (Fig. 4F, G, I). Phialides ampulliform to lageniform, often constricted below the tip to form a narrow neck, hyaline, (3.2–)3.5–7.0(–9.3) × (2.3–)2.6–3.3(–3.6) µm ($\bar{x}$ = 5.0 × 3.0 µm, n = 50), length/width ratio (1.2–)1.5–2.5(–4) ($\bar{x}$ = 1.8, n = 50), base 1.6–2.2 µm ($\bar{x}$ = 1.8 µm, n = 50) (Fig. 4I). Conidia subglobose to globose, smooth, hyaline when young, becoming green to dark green with age, (2.0–)2.3–2.7(–3.0) × (1.6–)2.0–2.6(–3.0) µm ($\bar{x}$ = 2.5 × 2.2 µm, n = 50), length/width ratio 1.0–1.3(–1.7) ($\bar{x}$ = 1.1, n = 50) (Fig. 4H). Chlamydospores unobserved. No odor; no diffusing pigment observed.

Additional specimen examined. China. Xixia District, Yinchuan, Ningxia Hui Autonomous Region, 38°38'52"N, 106°9'33"E, ca. 1127 m elev., from rhizosphere soil of *Lycium chinois*, 17 Oct 2018, Jing Z. Sun, living CGMCC 3.19697.

Teleomorph. Undetermined.

Note. Characterized by tree-like conidiophores, verticillate or in whorls of 3–4, ampulliform to lageniform phialides (3.5–7.0 × 2.6–3.4 µm), subglobose to globose conidia (2.2–2.6 × 2.0–2.4 µm). Differs from *Trichoderma lentinulae* by compact, relatively smaller phialides, and the character of pustules on SNA. Differs from *Trichoderma lixii* by shorter and wider phialides and smaller conidia.

***Trichoderma zelobreve* Jing Z. Sun & X.Z. Liu, sp. nov.**

MycoBank No: 833236

Fig. 5

Etymology. Greek *zelo*, meaning emulation + *breve*, referred to *Trichoderma breve*.

Type. China. Chaoyang District, Beijing, 40°0'41"N, 116°23'37"E, ca. 35 m elev., 19 Oct 2018, isolated from soil, Jing Z. Sun (HMAS 248254, holotype), ex-type culture CGMCC 3.19695.

Description. On CMD after 72 h, colony radius covering the plate at 25 °C and 30 °C, 11–12 mm at 35 °C. Colony hyaline, indistinctly radial; Aerial inconspicuous. No diffusing pigment, not distinct odor (Fig. 5B). Conidial production noted after

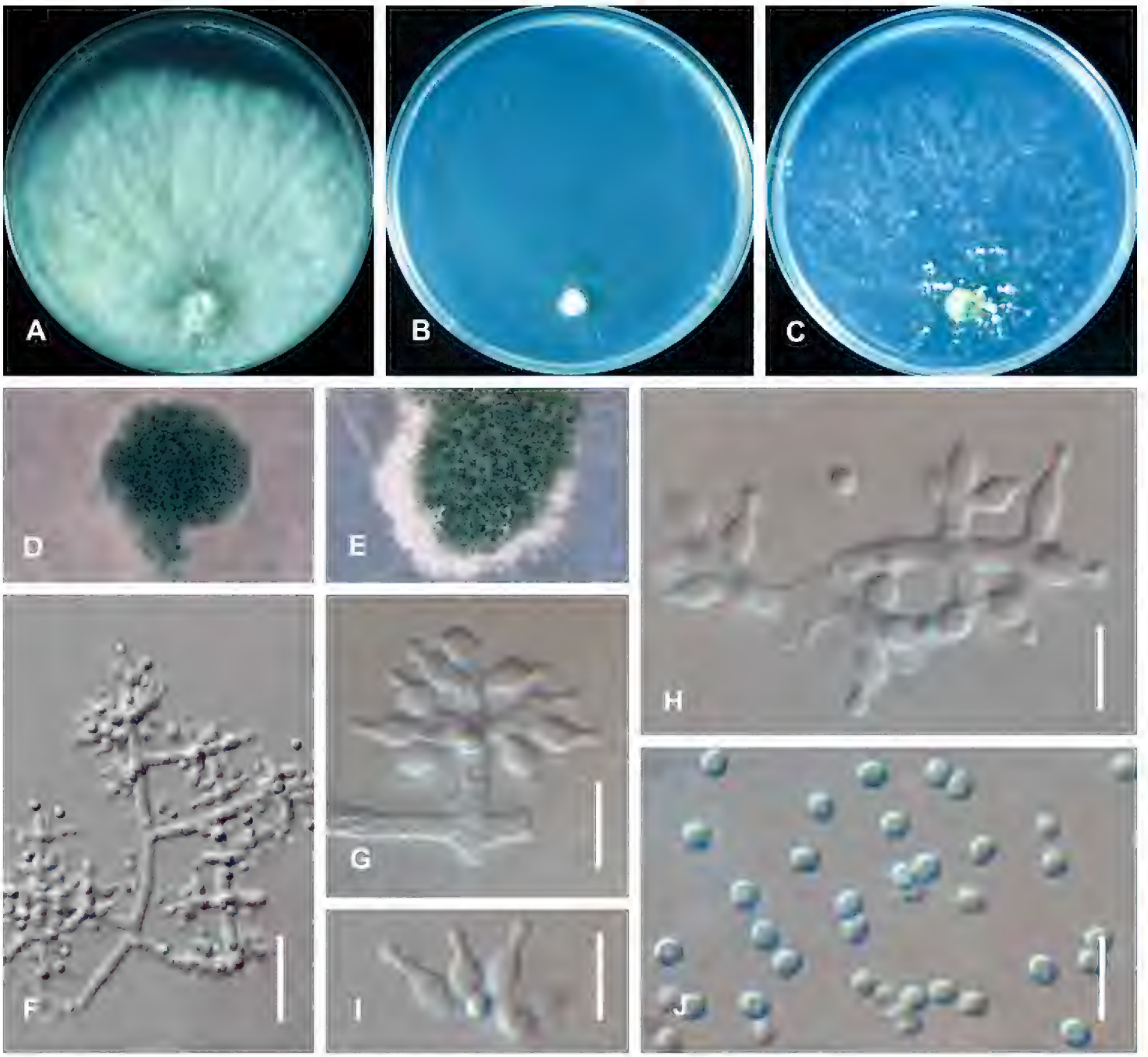

Figure 5. *Trichoderma zelobreve* (CGMCC 3.19695). Cultures at 25 °C after 3 days (**A** on PDA **B** on CMD **C** on SNA) **D** conidiation pustules on CMD after 10 days **E** conidiation pustules on SNA after 10 d **F** conidiophores **G, I** conidiophores and phialides **H** phialides with conidia **J** conidia. Scale bars: 25 μm (**F**); 10 μm (**G–J**).

5 days, starting around the original inoculum. Small pustules formed at the colony margin, first white, olivaceous after 6 d, with hairs protruding beyond the surface. Chlamydospores unobserved.

On PDA after 72 h, colony radius 55–58 mm at 25 °C, covering the plate at 30 °C, 8–9 mm at 35 °C. Colony white to yellow-white; mycelium dense and radial. Aerial conspicuous. No diffusing pigment, not distinct odor (Fig. 5A). Conidial production noted after 3 days, starting around the inoculum, effuse in the aerial hyphae, first white, turning green after 4 d. Chlamydospores unobserved.

On SNA after 72 h, colony radius 62–63 mm at 25 °C, covering the plate at 30 °C, 7–8 mm at 35 °C. Colony hyaline, regularly circular; mycelium loose. Aerial conspicuous. No diffusing pigment, not distinct odor (Fig. 5A). Conidial production noted after 2 days, starting around the inoculum, effuse in the aerial hyphae. Small pustules

formed along with two concentric rings, first white, turning yellow-green after 3 d, with hairs protruding beyond the surface. Conidiophores pyramidal with opposing branches, the distance between branches relatively large (Fig. 5F). Phialides, sometimes solitary, often paired or in whorls of 2–3 (Fig. 5F); whorls typically cruciate but often nearly verticillate; rarely conidiophores nodose and phialides disposed in more or less botryose clusters (Fig. 5G, H). Phialides ampulliform to lageniform, often constricted below the tip to form a narrow neck, hyaline (Fig. 5G, H, I), (3.5–)4.0–6.0(–7.0) × (2.2–)2.6–3.2(–3.5) μm ($\bar{x}$ = 4.8× 2.9 μm, n = 30), length/width ratio (1.1–)1.4–2.1(–2.5) ($\bar{x}$ = 1.5, n = 30), base 1.4–2.1 μm ($\bar{x}$ = 1.7 μm). Conidia ovoid to subglobose, smooth, hyaline when young, becoming green to dark green with age, (2.0–)2.3–2.6(–2.9) × (1.5–)1.8–2.2(–2.5) μm ($\bar{x}$ = 2.4 × 2.0 μm, n = 30), length/width ratio (0.8–)1.1–1.4(–1.7) ($\bar{x}$ = 1.2, n = 30) (Fig. 5J). Chlamydospores unobserved.

Additional specimen examined. China. Chaoyang District, Beijing, 40°0'41"N, 116°23'37"E, ca. 35 m elev., isolated from soil, 19 Oct 2018, Jing Z. Sun, living culture CGMCC 3.19696.

Teleomorph. Undetermined.

Note. Characterized by tree-like conidiophores, branches paired or in whorls of 3–4, ampulliform to lageniform (4.0–6.0 × 2.6–3.2 μm), ovoid to subglobose conidia (2.2–2.6 × 1.8–2.2 μm). Differs from *Trichoderma breve* by shorter phialides and smaller conidia, as well as the cultural characteristics and growth rates.

Discussion

A combination of phylogenetic, morphological, ecological, and biogeographical data has robustly resolved the taxonomy of *Trichoderma* (Jaklitsch and Voglmayr 2015; Qin and Zhuang 2016a; Sun et al. 2016; Chen and Zhuang 2017b; Qiao et al. 2018). In this study, phylogenetic analysis based on a single gene of ITS could not distinguish species of *Trichoderma* in the *Harzianum* clade from each other (Suppl. material 1: Fig. S1), which confirmed that the ITS region is not suitable for species delimitation of *Trichoderma* (Jaklitsch et al. 2012; Qin et al. 2018). Sequences of RPB2 and TEF1-α were powerful due to their suitable interspecific variations (Jaklitsch and Voglmayr 2015), and these have extensively been used in solving the taxonomy of *Trichoderma* (Jaklitsch and Voglmayr 2015; Qin and Zhuang 2016a; Chen and Zhuang 2017a, b; Qiao et al. 2018). Despite the phylogenetic analyses based on the single gene of RPB2 and TEF1-α generally revealed the phylogenetic relationship within the *Harzianum* clade (Suppl. material 1: Fig. S2, Suppl. material 3: Fig S3), but the relationships among *T. lentinulae*, *T. xixiacum*, *T. vermifimicola*, *T. zelobreve*, and their closed taxa were not well distinct. Consideration of the universality and reliability of barcodes for species in the *Trichoderma* genus (Qiao et al. 2018), combined ITS, RPB2, and TEF1-α dataset was used for phylogenetic analysis in this study, revealing phylogenetic relationship among species in *Harzianum* clades, and suggesting that *T. lentinulae*, *T. xixiacum*, *T. vermifimicola*, and *T. zelobreve* are distinguishable from each other and species within and outside of *Harzianum* clade as well.

Table 1. Species, strains and their corresponding GenBank accession numbers of sequences used for phylogenetic analyses.

Species	Voucher/ culture Nos.	Origin	Substrate	GenBank accession No.		
				ITS	RPB2	TEF1-a
Trichoderma afarasin	CBS 130755 ET	Cameroon	Soil	AY027784		AF348093
	DIS 314F	Cameroon	Wood	FJ442259	FJ442778	FJ463400
	GJS 06 98	Cameroon	Soil	FJ442630		FJ463327
Trichoderma afroharzianum	CBS 124620 ET	Peru	*Moniliophthora roreri*	FJ442265	FJ442691	FJ463301
	CBS 466.94	Netherlands		KP009262	KP009150	KP008851
	GJS 04-193	Cameroon	Soil	FJ442233	FJ442709	FJ463298
Trichoderma aggressivum	CBS 100525	UK	Mushroom compost	AF057600	AF545541	AF348095
	DAOM 222156 ET		Mushroom compost	AF456924	FJ442752	AF348098
	CBS 100526	Ireland	Mushroom compost	FJ442607	KP009166	KP008993
Trichoderma alni	CBS 120633 ET	UK, England	*Alnus glutinosa*	EU518651	EU498349	EU498312
	CPK 2494			EU518652	EU498350	EU498313
	HMAS 252890				KT343763	KT343758
Trichoderma alpinum	HMAS 248821 T	China, Sichuan	Soil	KY687906	KY687958	KY688012
	HMAS 248830			KY687912	KY687961	KY688015
	HMAS 248870			KY687953	KY687963	KY688017
Trichoderma amazonicum	CBS 126898 ET	Peru	*Hevea brasiliensis*	HM142358	HM142367	HM142376
	IB95			HM142359	HM142368	HM142377
	LA265			HM142360	HM142369	HM142379
Trichoderma atrobrunneum	GJS 05-101			FJ442677	FJ442745	FJ463392
	GJS 90-254			AF443926	FJ442735	AF443943
Trichoderma atrogelatinosum	BMCC LU498	New Zealand				KJ871087
	CBS 237.63 ET	New Zealand		MH858272	KJ842201	
	DAOM 167632					KJ871083
Trichoderma bannaense	HMAS 248840 T	China, Yunan	Soil	KY687923	KY687979	KY688037
	HMAS 248865			KY687948	KY688003	KY688038
Trichoderma breve	HMAS 248844 T	China, Beijing	Soil	KY687927	KY687983	KY688045
	HMAS 248845			KY687928	KY687984	KY688046
Trichoderma brevicrassum	HMAS 248871 T		Soil	KY687954	KY688008	KY688064
	HMAS 248872		Soil	KY687955	KY688009	KY688065
Trichoderma brunneoviride	CBS 120928			EU518661	EU498358	EU498318
	CBS 121130 ET			EU518659	EU498357	EU498316
Trichoderma camerunense	CBS 137272 ET	Cameroon	Soil	AY027780	–	AF348107
	GJS 99 231			AY027783		AF348108
Trichoderma catoptron	DAOM 232830				KJ842166	KJ871245
	GJS 02 76 ET	Sri Lanka	Wood	AY737766		AY737726
Trichoderma ceramicum	CBS 114576			FJ860743	FJ860531	FJ860628
Trichoderma cerinum	BMCC LU784					KJ871244
	DAOM 230012 ET	Nepal		KC171336	KJ842184	KJ871242
Trichoderma christiani	CBS 132572 ET	Spain			KJ665244	KJ665439
	S93				KJ665245	KJ665442
Trichoderma cinnamomeum	GJS 96-128				AY391916	AY391977
	GJS 97-233				AY391919	AY391978
Trichoderma cinnamomeum	GJS 97-237 ET	USA, Missour	Decaying wood	AY737759	AY391920	AY737732
Trichoderma compactum	CBS 121218			AY941822	KF134789	KF134798
Trichoderma concentricum	HMAS 248833 T	China, Hubei	Soil	KY687915	KY687971	KY688027
	HMAS 248858			KY687941	KY687997	KY688028
Trichoderma corneum	GJS 97-82 ET	Thailand			KJ665252	KJ665455
Trichoderma endophyticum	CBS 130729 ET	Ecuador	*Theobroma gileri*	FJ442243		FJ463319
	GS 2014a			FJ884177		FJ967822
Trichoderma epimyces	CBS 120534 ET	Austria		EU518663	EU498360	EU498320
	CPK 1980			EU518662	EU498359	EU498319
	CPK 2487 ET			EU518665	EU498361	EU498322

Species	Voucher/ culture Nos.	Origin	Substrate	GenBank accession No.		
				ITS	RPB2	TEF1-a
Trichoderma estonicum	GJS 96-129			AY737767	AF545514	AF534604
Trichoderma guizhouense	DAOM 231435			EF191296		EF191321
	HGUP0038 T			JN191311	JQ901400	JN215484
	S628				KJ665273	KJ665511
Trichoderma harzianum	CBS 226.95 ET	U.K.	Soil	AJ222720	AF545549	AF348101
	CBS 227.95			AF057605		AF348100
	GJS 05 107			FJ442679	FJ442708	FJ463329
	IMI 359823			EF113587		AF348092
Trichoderma hausknechtii	CBS 133493	France			KJ665276	KJ665515
Trichoderma helicolixii	CBS 133499 ET	Spain			KJ665278	KJ665517
Trichoderma helicolixii	CBS 135583				KJ665277	KJ665516
Trichoderma hengshanicum	HMAS 248852 T	China, Hubei	Soil	KY687935	KY687991	KY688054
	HMAS 248853			KY687936	KY687992	KY688055
Trichoderma hirsutum	HMAS 248834 T	China, Hubei	Soil	KY687916	KY687972	KY688029
	HMAS 248859			KY687942	KY687998	KY688030
Trichoderma hunanense	HMAS 248841 T	China, Hunan	Soil	NR_154571	KY687980	KY688039
	HMAS 248867			KY687950	KY688005	KY688040
Trichoderma ingratum	HMAS 248822 T	China, Sichuan	Soil	KY687917	KY687973	KY688018
	HMAS 248827			KY687909	KY687966	KY688021
	HMAS 248873			KY687956	KY688010	KY688022
Trichoderma inhamatum	CBS 273.78 ET	Colombia	Soil	FJ442680	FJ442725	AF348099
Trichoderma italicum	CBS 132567				KJ665282	KJ665525
	S15 ET	Italy			KJ665283	KJ665526
Trichoderma lentiforme	CBS 100542 ET	French Guiana	Decorticated wood	AF469189	–	AF469195
	DIS 253B			FJ442619	FJ442756	FJ851875
	DIS 94D			FJ442615	FJ442749	FJ463379
Trichoderma lentinulae	HMAS 248256 T	**China**	***Lentinula***	**MN594469**	**MN605867**	**MN605878**
	CGMCC 3.19848	**China**	***Lentinula***	**MN594470**	**MN605868**	**MN605879**
	CGMCC 3.19849	**China**	***Lentinula***	**MN594471**	**MN605869**	**MN605880**
	CGMCC 3.19699	**China**	**Soil**	**MN594478**	**MN605876**	**MN605887**
	CGMCC 3.19670	**China**	**Soil**	**MN594479**	**MN605877**	**MN605888**
Trichoderma liberatum	HMAS 248831 T	China,Hubei	Soil	KY687913	KY687969	KY688025
Trichoderma liberatum	HMAS 248832			KY687914	KY687970	KY688026
Trichoderma linzhiense	HMAS 248846 T	China, Tibet	Soil	KY687929	KY687985	KY688047
	HMAS 248874			KY687957	KY688011	KY688048
Trichoderma lixii	CBS 110080 ET	Thailand	Decayed *Ganoderma*	AF443920	KJ665290	AF443938
Trichoderma neotropicale	LA11 ET			HQ022407		HQ022771
	T51			FJ884180		FJ967825
Trichoderma parestonicum	CBS 120636 ET			FJ860803	FJ860565	
Trichoderma parepimyces	CBS 122768			FJ860801	FJ860563	FJ860665
	CBS 122769 ET	Austria	Wood	MH863234	FJ860562	FJ860664
Trichoderma perviride	HMAS 273786	China,Hubei	Wood		KX026962	KX026954
Trichoderma pinicola	KACC 48486 ET	Korea	root of Pinus densiflora	MH050354	MH025993	MH025981
	SFC20130926-S014				MH025991	MH025978
	SFC20130926-S111				MH025992	MH025980
Trichoderma pleuroti	CBS 124387 ET	Korea	*Pleurotus* substrate	HM142363	HM142372	HM142382
	CPK 2117					EU279975
Trichoderma pleuroticola	CBS 124383 ET	Korea	*Pleurotus* substrate	HM142362	HM142371	HM142381
	GJS 95 81			AF345948		AF348102
	TRS70 ET			KP009264	KP009172	KP008951
Trichoderma polypori	HMAS 248855 T	Hunan	Soil	KY687938	KY687994	KY688058
	HMAS 248861			KY687944	KY688000	KY688059
Trichoderma polysporum	S72					KJ665685

Species	Voucher/ culture Nos.	Origin	Substrate	GenBank accession No.		
				ITS	RPB2	TEF1-a
Trichoderma priscilae	CBS 131487 ET	Spain			KJ665333	KJ665691
Trichoderma pseudodensum	HMAS 248828 T	Hubei	Soil	KY687910	KY687967	KY688023
	HMAS 248829			KY687911	KY687968	KY688024
Trichoderma pseudogelatinosum	CNUN309 ET	Japan	Shiitake mushroom	HM769754	HM920173	HM920202
Trichoderma purpureum	HMAS 273787 T	China,Hubei			KX026961	KX026953
Trichoderma pyramidale	CBS 135574 ET	Italy	*Olea europaea*		KJ665334	KJ665699
Trichoderma rifaii	CBS 130746	Ecuador	*Theobroma gileri*	FJ442663		FJ463324
	DIS 337F ET			FJ442621	FJ442720	FJ463321
Trichoderma rufobrunneum	HMAS 266614 T	China,Jilin	Rotten wood	KF729998	KF730010	KF729989
	isolate 8155				KF730007	KF729992
Trichoderma rugulosum	SFC20180301-001 T			MH050353	MH025986	MH025984
	SFC20180301-002				MH025987	MH025985
Trichoderma simmonsii	CBS 130431	USA, Maryland	Decaying wood bark	AF443917	FJ442757	AF443935
	S297					KJ665711
	S7				KJ665337	KJ665719
Trichoderma simplex	HMAS 248842 T	China, Guangxi	Soil	KY687925	KY687981	KY688041
	HMAS 248860			KY687943	KY687999	KY688042
Trichoderma solum	HMAS 248847			KY687930	KY687986	KY688049
	HMAS 248848 T	China, Hubei	Soil	KY687931	KY687987	KY688050
	HMAS 248849			KY687932	KY687988	KY688051
Trichoderma stramineum	CBS 114248 ET	Sri Lanka	Decaying wood	AY737765	AY391945	AY737746
	TAMA 0425			AB856609	AB856748	AB856675
Trichoderma tawa	CBS 114233 ET	Thailand	Decaying bark	AY737756	AY391956	FJ463313
	DAOM 232841				KJ842187	EU279972
Trichoderma tenue	HMAS 273785 ET	China,Hubei	Wood		KX026960	KX026952
Trichoderma tomentosum	DAOM 171918			AY605715		AY605759
	DAOM 178713a ET	Canada, Ontario	*Ulmus* wood	EU330958	AF545557	AY750882
	DAOM 234236			EU280083		EU279971
Trichoderma velutinum	DAOM 230013 ET	Nepal	Soil	AF149873	JN133569	AY937415
	HMAS 273865 T	China, Heilongjiang	Soil		KX026965	KX026957
Trichoderma vermifimicola	**CGMCC 3.19850**	**China**	**Compost**	**MN594472**	**MN605870**	**MN605881**
	HMAS 248255 T	**China**	**Compost**	**MN594473**	**MN605871**	**MN605882**
Trichoderma xixiacum	**HMAS 248253** T	**China**	**Soil**	**MN594476**	**MN605874**	**MN605885**
	CGMCC 3.19698	**China**	**Soil**	**MN594477**	**MN605875**	**MN605886**
Trichoderma zayuense	HMAS 248835 T	China,Tibet	Soil	KY687918	KY687974	KY688031
	HMAS 248836			KY687919	KY687975	KY688032
Trichoderma zelobreve	**HMAS 248254** T	**China**	**Mushroom**	**MN594474**	**MN605872**	**MN605883**
	CGMCC 3.19696	**China**	**Soil**	**MN594475**	**MN605873**	**MN605884**
Trichoderma zeloharzianum	YMF 1.00268 ET	China,Yunan	Soil	MH113932	MH158996	MH183181

Trichoderma lentinulae was phylogenetically close to *T. xixiacum* and *T. lixii* but represents a taxon (Fig. 1). Morphologically, it differed from *T. xixiacum* in producing less frequently lageniform phialides with inequilateral to a strongly-curved apex. The conidia of *T. lentinulae* are usually more slender ($\bar{x}$ = 2.0), than those of *T. xixiacum* ($\bar{x}$ = 1.8). In addition, the conidia of *T. lentinulae* (length/width ratio, $\bar{x}$ = 1.2) are slightly more slender than *T. xixiacum* (length/width ratio, $\bar{x}$ = 1.1). The two species also differ from each other in their cultural characteristics and growth rates (Figs 2A–C, 4 A–C). *Trichoderma lentinulae* differed from *T. lixii* in producing less fre-

quently lageniform phialide with inequilateral to a strongly-curved apex. Additionally, *T. lentinulae* forms 2–5 apex phialides on the main axis (Fig. 2F, I) in contrast to 2–4 apex phialides of *T. lixii* (Chaverri et al. 2015). *Trichoderma lentinulae* is also clearly distinguished from *T. lixii* (phialides, 6.5–3.5 µm; conidia, 3.0–2.7 µm)(Chaverri et al. 2015) in producing shorter phialides ($\bar{x}$ = 4.5 × 3.0 µm) and smaller conidia ($\bar{x}$ = 2.5 × 2.2 µm). *Trichoderma vermifimicola* was phylogenetically associated with *T. simmonsii* (Fig. 1). Morphologically, it is hard to distinguish *T. vermifimicola* from *T. simmonsii* , because both form similar tree-like conidiophores, ampulliform to lageniform phialides and ovoid to subglobose conidia, but phialide whorls of *T. vermifimicola* were often nearly verticillate rather than cruciate in *T. simmonsii* (Chaverri et al. 2015). Furthermore, *T. simmonsii* grew fast (PDA 25–55 mm, SNA 10–35 mm) at 35 °C than *T. vermifimicola*. Additionally, the length/width ratio phialide of *T. vermifimicola* is larger ($\bar{x}$ = 2.4) than that of *T. simmonsii* ($\bar{x}$ = 1.9) (Chaverri et al. 2015), and *T. vermifimicola* also produces smaller conidia ($\bar{x}$ = 2.4 × 2.2 µm) (Fig. 3) than *T. simmonsii* (3.0–2.7 µm) (Chaverri et al. 2015). *Trichoderma zelobreve* was closely related to *Trichoderma breve* in the multi-gene phylogenetic analysis (Fig. 1). Morphologically, both fungi have short phialides, however, *T. zelobreve* differs from *T. breve* by producing shorter and narrower phialides (4.0–6.0 × 2.6–3.2 µm) than that of *T. breve* (6.7–10.0 × 2.8–3.9 µm) (Chen and Zhuang 2017a). The conidia of *T. zelobreve* are smaller ($\bar{x}$ = 2.4 × 2.0 µm) than those of *T. breve* ($\bar{x}$ = 3.0 × 2.8 µm). Additionally, *T. zelobreve* does not form a zonate colony on CMD, PDA, and SNA, whereas the colony of *T. breve* presents concentric zones on CMD and PDA and finely concentric zones on SNA (Chen and Zhuang 2017a). In a previous study, the phylogenetic analysis indicated that *T. breve* was a sister taxon of *T. bannaense*, but morphologically more similar to *T. harzianum* (Chen and Zhuang (2017a). Herein, our phylogenetic analyses presented *T. breve* was associated with *T. zelobreve* (Fig. 1), resulted from the little genetic variation of sequences of ITS and TEF1-α between them. The phylogenetic analysis in Chaverri et al. (2015) presented that *T. simmonsii* was associated with *T. camerunense*. In this study, our phylogenetic analysis presented that *T. simmonsii* was phylogenetically closed to *T. vermifimicola*, and *T. camerunense* phylogenetic to *T. rifaii* (Fig 1, Suppl. material 3: Fig S3). In a previous study, these species were recognized as the cryptic species in under *T. harzianum* (Chaverri et al. (2015).

Currently, the *Harzianum* clade contains more than 60 species which were isolated from soil, plant tissues, and other fungi (Jaklitsch and Voglmayr 2015; Qin and Zhuang 2016a; Chen and Zhuang 2017b; Qiao et al. 2018; Sun et al. 2019a, b). Several studies have confirmed that species in this clade are important because of their mycoparasitism (Chaverri et al. 2015; Chen and Zhuang 2017a; Sun et al. 2019). When numerous biological control agents were explored deriving from species in the *Harzianum* clade (Chaverri et al. 2015, several taxa, such as *T. atrobrunneum T. pleuroti*, and *T. pleuroticola* were recognized as causing agents of "Green mold" disease of cultivated mushroom (Innocenti et al. 2019; Sun et al. 2019a, b). In this study, *T. lentinulae* was isolated from a fruiting body and the cultivated substrates of *L. edodes*, causing the decay of the host as well. How *T. lentinulae* affect the cultivation of *Lentinula edodes* is worthy of further studies. Since *T. lentinulae* was isolated from mushroom, *T. lentinulae* and *T. vermifimicola*

were isolated from the mushroom spawn and substrates for earthworm cultivation, *T. xixiacum* and *T. zelobreve* were isolated from soil, confirming that species in the *Harzianum* clade have flexible nutrition modes (Chaverri and Samuels 2013; Zhang et al. 2018). The new species introduced here are not only potential candidates for biological agent exploration, but also improve our understanding of the diversity of *Trichoderma*, especially of the *Harzianum* clade in China.

Acknowledgements

This research was jointly supported by Key Research and Development Programs in Ningxia Hui Autonomous Region (2018BBF02004) and the Natural Science Foundation of China (no. 31600024).

References

Atanasova L, Druzhinina IS, Jaklitsch WM, Mukherjee P, Horwitz B, Singh U (2013) Two hundred *Trichoderma* species recognized on the basis of molecular phylogeny. *Trichoderma*: Biology and Applications CABI, Wallingford: 10–42. https://doi.org/10.1079/9781780642475.0010

Bunbury-Blanchette AL, Walker AK (2019) *Trichoderma* species show biocontrol potential in dual culture and greenhouse bioassays against *Fusarium* basal rot of onion. Biological Control 130: 127–135. https://doi.org/10.1016/j.biocontrol.2018.11.007

Carbone I, Kohn LM (1999) A method for designing primer sets for speciation studies in filamentous ascomycetes. Mycologia 91: 553–556. https://doi.org/10.1080/00275514.1999.12061051

Castresana J (2000) Selection of conserved blocks from multiple alignments for their use in phylogenetic analysis. Molecular Biology and Evolution 17: 540–552. https://doi.org/10.1093/oxfordjournals.molbev.a026334

Chaverri P, Branco-Rocha F, Jaklitsch W, Gazis R, Degenkolb T, Samuels GJ (2015) Systematics of the *Trichoderma harzianum* species complex and the re-identification of commercial biocontrol strains. Mycologia 107: 558–590. https://doi.org/10.3852/14-147

Chaverri P, Samuels GJ (2013) Evolution of habitat preference and nutrition mode in a cosmopolitan fungal genus with evidence of interkingdom host jumps and major shifts in ecology. Evolution 67: 2823–2837. https://doi.org/10.1111/evo.12169

Chen K, Zhuang WY (2016) *Trichoderma shennongjianum* and *Trichoderma tibetense*, two new soil-inhabiting species in the Strictipile clade. Mycoscience 57: 311–319. https://doi.org/10.1016/j.myc.2016.04.005

Chen K, Zhuang WY (2017a) Discovery from a large-scaled survey of *Trichoderma* in soil of China. Scientific Reports 7, 9090. https://doi.org/10.1038/s41598-017-07807-3

Chen K, Zhuang WY (2017b) Three new soil-inhabiting species of *Trichoderma* in the Stromaticum clade with test of their antagonism to pathogens. Current Microbiology 74: 1049–1060. https://doi.org/10.1007/s00284-017-1282-2

Cunningham CW (1997) Can three incongruence tests predict when data should be combined? Molecular Biology and Evolution 14: 733–740. https://doi.org/10.1093/oxfordjournals.molbev.a025813

Degenkolb T, Nielsen KF, Dieckmann R, Branco-Rocha F, Chaverri P, Samuels GJ, Thrane U, von Dohren H, Vilcinskas A, Bruckner H (2015) Peptaibol, secondary-metabolite, and hydrophobin pattern of commercial biocontrol agents formulated with species of the *Trichoderma harzianum* Complex. Chemistry & Biodiversity 12: 662–684. https://doi.org/10.1002/cbdv.201400300

Druzhinina IS, Kopchinskiy AG (2006) TrichOKEY v. 2 – A DNA Oligonucleotide BarCode Program for the Identification of Multiple Sequences of Hypocrea and Trichoderma. In: Meyer W, Pearce C (Eds) International Proceedings of the 8th International Mycological Congress. Cairns, Australia, Medimond, Bologna, Italy.

Druzhinina IS, Kopchinskiy AG, Komoń M, Bissett J, Szakacs G, Kubicek CP (2005) An oligonucleotide barcode for species identification in *Trichoderma* and *Hypocrea*. Fungal Genetics and Biology 42: 813–828. https://doi.org/10.1016/j.fgb.2005.06.007

du Plessis IL, Druzhinina IS, Atanasova L, Yarden O, Jacobs K (2018) The diversity of *Trichoderma* species from soil in South Africa, with five new additions. Mycologia 110: 559–583. https://doi.org/10.1080/00275514.2018.1463059

Gazis R, Chaverri P (2010) Diversity of fungal endophytes in leaves and stems of wild rubber trees (Hevea brasiliensis) in Peru. Fungal Ecology 3: 240–254. https://doi.org/10.1016/j.funeco.2009.12.001

Innocenti G, Montanari M, Righini H, Roberti R (2019) *Trichoderma* species associated with green mould disease of *Pleurotus ostreatus* and their sensitivity to prochloraz. Plant Pathology 68: 392–398. https://doi.org/10.1111/ppa.12953

Jaklitsch WM, Komon M, Kubicek CP, Druzhinina IS (2005) *Hypocrea voglmayrii* sp. nov. from the Austrian Alps represents a new phylogenetic clade in *Hypocrea*/*Trichoderma*. Mycologia 97: 1365–1378. https://doi.org/10.1080/15572536.2006.11832743

Jaklitsch WM, Voglmayr H (2015) Biodiversity of *Trichoderma* (Hypocreaceae) in southern Europe and Macaronesia. Studies in Mycology 80: 1–87. https://doi.org/10.1016/j.simyco.2014.11.001

Jiang Y, Wang JL, Chen J, Mao LJ, Feng XX, Zhang CL, Lin FC (2016) *Trichoderma* biodiversity of agricultural fields in East China reveals a gradient distribution of species. PLoS ONE 11(8): e0160613. https://doi.org/10.1371/journal.pone.0160613

Katoh K, Standley DM (2013) MAFFT Multiple sequence alignment software version 7: improvements in performance and usability. Molecular Biology and Evolution 30: 772–780. https://doi.org/10.1093/molbev/mst010

Kopchinskiy A, Komoń M, Kubicek CP, Druzhinina IS (2005) TrichoBLAST: a multilocus database for *Trichoderma* and *Hypocrea* identifications. Mycological Research 109: 658–660. https://doi.org/10.1017/S0953756205233397

Liu YJJ, Whelen S, Benjamin DH (1999) Phylogenetic relationships among ascomycetes: Evidence from an RNA polymerase II subunit. Molecular Biology and Evolution 16: 1799–1808. https://doi.org/10.1093/oxfordjournals.molbev.a026092

Nylander JAA (2004) MrModeltest v2. Program distributed by the author. Evolutionary Biology Centre, Uppsala University. https://github.com/nylander/MrModeltest2

Phookamsak R, Hyde KD, Jeewon R, Bhat DJ, Jones EBG, Maharachchikumbura SSN, Raspé O, Karunarathna SC, Wanasinghe DN, Hongsanan S, Doilom M, Tennakoon DS, Machado AR, Firmino AL, Ghosh A, Karunarathna A, Mešić A, Dutta AK, Thongbai B, Devadatha B, Norphanphoun C, Senwanna C, Wei D, Pem D, Ackah FK, Wang GN, Jiang HB, Madrid H, Lee HB, Goonasekara ID, Manawasinghe IS, Kušan I, Cano J, Gené J, Li J, Das K, Acharya K, Raj KNA, Latha KPD, Chethana KWT, He MQ, Dueñas M, Jadan M, Martín MP, Samarakoon MC, Dayarathne MC, Raza M, Park MS, Telleria MT, Chaiwan N, Matočec N, de Silva NI, Pereira OL, Singh PN, Manimohan P, Uniyal P, Shang QJ, Bhatt RP, Perera RH, Alvarenga RLM, Nogal-Prata S, Singh SK,Vadthanarat S, Oh SY, Huang SK, Rana S, Konta S, Paloi S, Jayasiri SC, Jeon SJ, Mehmood T, Gibertoni TB, Nguyen TTT, Singh U, Thiyagaraja V, Sarma VV, Dong W, Yu XD, Lu YZ, Lim YW, Chen Y, Tkalčec Z, Zhang ZF, Luo ZL, Daranagama DA, Thambugala KM, Tibpromma S, Camporesi E, Bulgakov T, Dissanayake AJ, Senanayake IC, Dai DQ, Tang LZ, Khan S, Zhang H, Promputtha I, Cai L, Chomnunti P, Zhao RL, Lumyong S, Boonmee S, Wen TC, Mortimer PE, Xu J (2019) Fungal diversity notes 929–1036: taxonomic and phylogenetic contributions on genera and species of fungal taxa. Fungal Diversity 95: 1–273. https://doi.org/10.1007/s13225-019-00421-w

Qiao M, Du X, Zhang Z, Xu JP, Yu ZF (2018) Three new species of soil-inhabiting *Trichoderma* from southwest China. Mycokeys: 63–80. https://doi.org/10.3897/mycokeys.44.30295

Qin WT, Zhuang WY (2016a) Four new species of *Trichoderma* with hyaline ascospores from central China. Mycological Progress 15: 811–825. https://doi.org/10.1007/s11557-016-1211-y

Qin WT, Zhuang WY (2016b) Two new hyaline-ascospored species of Trichoderma and their phylogenetic positions. Mycologia 108: 205–214. https://doi.org/10.3852/15-144

Qin WT, Zhuang WY (2017) Seven new species of *Trichoderma* (Hypocreales) in the Harzianum and Strictipile clades. Phytotaxa 305: 121–139. https://doi.org/10.11646/phytotaxa.305.3.1

Rambaut A (2012) FigTree v1. 4. Molecular evolution, phylogenetics and epidemiology. Edinburgh: University of Edinburgh, Institute of Evolutionary Biology.

Ronquist F, Teslenko M, van der Mark P, Ayres DL, Darling A, Hohna S, Larget B, Liu L, Suchard MA, Huelsenbeck JP (2012) MrBayes 3.2: efficient Bayesian phylogenetic inference and model choice across a large model space. Systematic Biology 61: 539–542. https://doi.org/10.1093/sysbio/sys029

Stamatakis A (2006) RAxML-VI-HPC: maximum likelihood-based phylogenetic analyses with thousands of taxa and mixed models. Bioinformatics 22: 2688–2690. https://doi.org/10.1093/bioinformatics/btl446

Sun JZ, Liu XZ, Jeewon R, Li YL, Lin CG, Tian Q, Zhao Q, Xiao XP, Hyde KD, Nilthong S (2019a) Fifteen fungicolous Ascomycetes on edible and medicinal mushrooms in China and Thailand. Asian Journal of Mycology 2(1): 129–169. https://doi.org/10.5943/ajom/2/1/7

Sun JZ, Liu XZ, McKenzie EH, Jeewon R, Liu JK, Zhang XL, Zhao Q, Hyde KD (2019b) Fungicolous fungi: terminology, diversity, distribution, evolution, and species checklist. Fungal Diversity 95(1): 337–430. https://doi.org/10.1007/s13225-019-00422-9

Sun RY, Liu ZC, Fu KH, Fan LL, Chen J (2012) *Trichoderma* biodiversity in China. Journal of Applied Genetics 53: 343–354. https://doi.org/10.1007/s13353-012-0093-1

Sun JZ, Pei YF, Li EW, Li W, Hyde KD, Yin WB, Liu XZ (2016) A new species of *Trichoderma hypoxylon* harbours abundant secondary metabolites. Scientific Reports 6, 37369. https://doi.org/10.1038/srep37369

White T, Bruns T, Lee S, Taylor J (1990) Amplification and direct sequencing of fungal ribosomal RNA genes for phylogenetics In: Innis MA, Gelfand DH, Sninsky JJ, White TJ (Eds) PCR protocols: a guide to methods and applications, 315–322. https://doi.org/10.1016/B978-0-12-372180-8.50042-1

Zhang WW, Zhang XL, Li K, Wang CS, Cai L, Zhuang WY, Xiang M, Liu XZ (2018) Introgression and gene family contraction drive the evolution of lifestyle and host shifts of hypocrealean fungi. Mycology 9: 176–188. https://doi.org/10.1080/21501203.2018.1478333

Zhang YJ, Zhang S, Liu XZ, Wen HA, Wang M (2010) A simple method of genomic DNA extraction suitable for analysis of bulk fungal strains. Letters in applied microbiology 51(1): 114–118. https://doi.org/10.1111/j.1472-765X.2010.02867.x

Zhu ZX, Zhuang WY (2015) *Trichoderma* (Hypocrea) species with green ascospores from China. Persoonia 34: 113–129. https://doi.org/10.3767/003158515X686732

Supplementary material 1

Figure S1

Authors: Xin Gu, Rui Wang, Quan Sun, Bing Wu, Jing-Zu Sun

Data type: phylogenetic tree

Explanation note: Phylogenetic tree based on Maximum Likelihood analysis of ITS sequence dataset. *Trichoderm ceramicum*, *Trichoderma estonicum*, and *Trichoderm parastinicum* were chosen as the outgroup. Bootstrap Values higher than 70% from RAxML (BSML) (left) and Bayesian posterior probabilities greater than 0.95 (BYPP) (right) are given above the nodes. ^{T} indicates the type; ^{ET} indicates the ex-living type. Isolates obtained in this study are in red.

Copyright notice: This dataset is made available under the Open Database License (http://opendatacommons.org/licenses/odbl/1.0/). The Open Database License (ODbL) is a license agreement intended to allow users to freely share, modify, and use this Dataset while maintaining this same freedom for others, provided that the original source and author(s) are credited.

Link: https://doi.org/10.3897/mycokeys.73.51424.suppl1

Supplementary material 2

Figure S2

Authors: Xin Gu, Rui Wang, Quan Sun, Bing Wu, Jing-Zu Sun

Data type: phylogenetic tree

Explanation note: Phylogenetic tree based on Maximum Likelihood analysis of RPB2 sequence dataset. *Trichoderm ceramicum*, *Trichoderma estonicum*, and *Trichoderm parastinicum* were chosen as the outgroup. Bootstrap Values higher than 70% from RAxML (BSML) (left) and Bayesian posterior probabilities greater than 0.95 (BYPP) (right) are given above the nodes. [T] indicates the type; [ET] indicates the ex-living type. Isolates obtained in this study are in red

Copyright notice: This dataset is made available under the Open Database License (http://opendatacommons.org/licenses/odbl/1.0/). The Open Database License (ODbL) is a license agreement intended to allow users to freely share, modify, and use this Dataset while maintaining this same freedom for others, provided that the original source and author(s) are credited.

Link: https://doi.org/10.3897/mycokeys.73.51424.suppl2

Supplementary material 3

Figure S3

Authors: Xin Gu, Rui Wang, Quan Sun, Bing Wu, Jing-Zu Sun

Data type: phylogenetic tree

Explanation note: Phylogenetic tree based on Maximum Likelihood analysis of TEF1α sequence dataset. *Trichoderm ceramicum* was chosen as the outgroup. Bootstrap Values higher than 70% from RAxML (BSML) (left) and Bayesian posterior probabilities greater than 0.95 (BYPP) (right) are given above the nodes. [T] indicates the type; [ET] indicates the ex-living type. Isolates obtained in this study are in red.

Copyright notice: This dataset is made available under the Open Database License (http://opendatacommons.org/licenses/odbl/1.0/). The Open Database License (ODbL) is a license agreement intended to allow users to freely share, modify, and use this Dataset while maintaining this same freedom for others, provided that the original source and author(s) are credited.

Link: https://doi.org/10.3897/mycokeys.73.51424.suppl3